



**Scottish Universities Environmental Research Centre**

**Luminescence Dating  
of Sediments from  
Droughduil Mound, Dunragit**

**2004**



**D.C.W. Sanderson, I.M.C Anthony & C. Kerr**

---

**East Kilbride Glasgow G75 0QF Telephone: 01355 223332 Fax: 01355 229898**

---

**Luminescence Dating of Sediments from Droughduil  
Mound, Dunragit, Dumfriesshire**

**2004**

**D.C.W. Sanderson, I.M.C Anthony, C Kerr**

**Scottish Universities Environmental Research Centre,  
East Kilbride G75 0QF**

## Summary

This report presents details of the application of Optically Stimulated Luminescence (OSL) dating sediments from Droughduil mound, Dunragit. OSL dating operates by measuring the intensity of luminescence signals which are induced by long term exposure of minerals such as quartz to ionising radiation in the environment. OSL signals are bleached by exposure to daylight, and build up while the sample is enclosed in the archaeological monument. Providing the sample has been reset at time of deposition, the combination of OSL measurements of the radiation dose received and assessment of the environmental radioactivity of the sample and its context can be used to date depositional events.

A series of samples were collected from Droughduil mound during a site visit on 29<sup>th</sup> August 2002. A total of eleven dating samples were collected from exposed sections using plastic tubing, and accompanied by in-situ measurements of the local gamma radiation fields of the site were used for dating measurements. Bulk samples were also collected for the purpose of laboratory gamma spectrometry .

The quartz single-aliquot regenerative OSL dating procedure was applied successfully to all eleven samples. Radiation dosimetry combined field gamma spectrometry, thick source beta counting and high resolution gamma spectrometry. In all cases it was possible to use the OSL data to determine equivalent doses for the samples.

A stratified sequence of dates were obtained from the base of the mound, indicating past land use stretching back to the mid 3<sup>rd</sup> millenium BC. Material collected from contexts thought to predate the cairn construction on the site, and others thought to post-date the cairn collapse, suggest construction and use of the cairn in the mid-late 2<sup>nd</sup> millenium BC.

## **Contents**

1. Introduction	1
2. Background	1
3. Sampling	2
3.1 Sampling trip	2
4. Luminescence Analysis	4
4.1 Sample Preparation	4
4.2 Measurements	4
4.2.1 Dose Rate Measurements	4
4.2.2 Luminescence measurements	5
5. Results	7
5.1 Dose Rate Measurements and Calculations	7
5.2 Single Aliquot OSL Results	10
6. Discussion and conclusions	12
7. References	15

## List of Tables

Table 3.1	Sampling and gamma dosimetry details for OSL tube samples	3
Table 5.1	Activity and Equivalent concentrations of K, U and Th for samples SUTL1435-1445 as determined by HRGS	8
Table 5.2	Dose Rates Determined by HRGS, TSBC and field gamma measurements	8
Table 5.3	Annual Dose Rates for samples SUTL1435-1445	9
Table 5.4	Summary of SAR results from 16 disc runs	11
Table 5.5	Summary of Age estimates	12
Table 6.1	Final Age Estimates	13

## List of figures

Fig 4.1	Quartz Single Aliquot Regenerative Sequence	6
Fig 6.1	North Facing Section of Droughduil mound, indicating position of samples SUTL 1439-1444 and dating results	14

## 1. Introduction

This report presents sampling details and results of investigations of optically stimulated luminescence (OSL) from sediment samples recovered from Droughduil mound, Dunragit, Dumfriesshire, during excavations conducted Manchester University.

## 2. Background

A sampling visit to Dunragit mound was undertaken on 28<sup>th</sup> August to facilitate luminescence dating of sediments. The mound has a spatial alignment with the entrance ways to middle and outer circles in a nearby field, identified from aerial photography, and partially excavated. It has been postulated that the mound may also be of pre-historic (ie late Neolithic/early bronze age) origins, rather than a medieval Motte-like object, in which case it may have had a role connected with the activities in the henge-like monuments to which it appears linked. The purpose of the sampling trip was to identify opportunities for optically stimulated luminescence (OSL) dating of sediments which might be helpful in clarifying the formation chronology of the monument.

OSL dating records the luminescence levels induced by exposure to natural background radiation during periods of enclosure and protection from daylight. Quartz and feldspars, which are both common components of most sands and sediments are capable of accumulating luminescence signals. For dating purposes we require a depositional history which deposited the sediment with negligible residual levels of luminescence. OSL signals from quartz, and feldspars are rapidly depleted by exposure to daylight. Typical bleaching rates result in 3 orders of magnitude signal reduction in  $10^6$ - $10^7$  J m<sup>-2</sup> exposure to daylight, which can be readily achieved at UK latitudes in less than a single day. Therefore sedimentary deposition processes which result on significant exposure to daylight immediately prior to deposition, or to enclosure of sediments whose recent environmental history of erosion and transport has already resulted in negligible residuals, can provide the basis for meaningful dating. In practice Aeolian sediments are normally expected to be well bleached. Other classes of sediments may experience more complex depositional histories, which can lead to mixed age material, or to partially bleached samples. While luminescence characterisation of such re-deposited materials may also be of value in understanding the formation history of archaeological sites, dating may be problematical in the absence of a well constrained depositional event.

At the time of the visit, the excavation had progress to the extent of revealing two structures in the upper area: (i) the remains of a mortared structure which contained a document indicating demolition of an observational hut in the early 20<sup>th</sup> century, (ii) a stone cairn presumed to be of prehistoric origins and containing quantities of burned bone. A section from the top to the bottom of the site in the lee side showed extensive evidence of wind-blown sand. Indeed the cairn was set on relatively clean sand, and a layer of stones, presumed to be associated with the collapse of the cairn could be seen in section particularly at the top and bottom of the mounds. This collapse layer was also enclosed above, and below by windblown sands. At the base of the mound the sand layers continued with vestigial remains of possible weathered landscape surfaces (revealed by oxidation stains) and darker layers that may have represented older

vegetation layers. While it was difficult to identify a palaeolandscape surface that predated the original mound, opportunities were identified for sampling Aeolian sands that should represent (i) the landscape evolution in the earlier formation stages of the mound, (ii) layers that predate the construction of the cairn, (iii) layers that predate the cairn collapse, and layers that post date the major collapse of the cairn.

### **3. Sampling**

#### **3.1 Sampling trip**

Eleven samples for OSL dating were collected during the fieldtrip from selected locations. In each case the area was cleaned back immediately prior to sampling to remove layers which may have been bleached by excavation. Samples were collected in opaque 4 cm diameter tubes, which were removed by overcutting the sampling location with a 10 cm diameter black pipe. The sample tubes were transferred to lightproof bags, endcapped, labelled and sealed to retain moisture. Gamma ray spectra were recorded in the sampling location using a 50mmx50mm NaI detector and Rainbow 1000 channel spectrometer. Integral count rates above 450 keV were converted to gamma dose rates using conversion factors determined at the SUERC gamma ray calibration facility in East Kilbride. The samples have been registered in the SUERC luminescence laboratory and weighed to establish a traceable water content history. They are currently dark stored pending selection for measurement. Site coordinates for each sampling location were recorded, and the locations transcribed to site records.

Of the eleven samples, four represent the material under the edges and centre of the cairn. One mid-slope sample predates the collapse of the cairn and should record a period associated with the construction of either the main mound, or the cairn. At the base of the mound a set of 6 vertically stratified samples has also been assembled which represent the full sequence of events revealed by the excavation. The set contains sufficient replicates to provide internal consistency checks on dating assumptions. A small quantity of sand was also collected from superficial areas around the excavation for use as a modern bleaching control.

OSL No.	Co-ord		Description of Context	SUTL No.	In situ $\gamma$ dose rate (mGya <sup>-1</sup> )	Significance
1	E	528.328	10cm beneath cairn	1435	0.318±0.015	Tpq for cairn
	N	468.327				
2	E	528.318	28cm below cairn	1436	0.276±0.015	Predates OSL 1
	N	468.340				
3	E	528.250	Base of cairn in sand/cobbles	1437	0.342±0.015	Tpq for end of cairn
	N	468.170				
4	E	523.488	Beneath stones, mound side	1438	0.276±0.015	Tpq for collapse
	N	466.104				
5	E	511.570	Bottom profile, above stone layer	1439	0.293±0.015	Tpq for cairn collapse
	N	466.077				
6	E	511.587	Below stone layer	1440	0.313±0.015	Tpq for cairn collapse
	N	466.074				
7	E	511.599	Below first 'turf' feature – Earlier land surface	1441	0.284±0.015	Earlier land surface
	N	466.090				
8	E	511.617	Below 2 <sup>nd</sup> 'turf' feature – Earlier land surface	1442	0.280±0.015	Earlier land surface
	N	466.123				
9	E	511.642	Below weathered surface features – Earlier land surface	1443	0.273±0.015	Earlier land surface
	N	466.071				
10	E	511.632	Base of Trench- oldest excavated layer	1444	0.257±0.015	Oldest excavated layer
	N	466.128				
11	E	529.810	Beneath cairn after quarter sectioning	1445	0.331±0.015	Beneath cairn after quarter sectioning
	N	467.722				

**Table 3.1 Sampling and gamma dosimetry details for OSL tube samples**

## **4. Luminescence Analysis**

### **4.1 Sample Preparation**

Mineral extraction for all samples was aimed at recovery of quartz for analysis by the single aliquot regenerative (SAR) OSL method, and of measurement of dose rates from the sample material to facilitate age estimation. The first step was to measure the initial, dry and saturated weights of each sample to determine actual and saturated water contents. Samples were then removed from the tubes, dried at 50°C and then split to remove 20-50 g of material for dose rate measurements. The remaining material was sieved to recover 90-120µm and 120-250µm size fractions. These were treated with 1M HCl for 30 minutes, then for 40 minutes with 40% HF, followed by a further 30 min 1M HCl treatment then centrifuged in sodium polytungstate solution to remove heavy minerals with densities greater than 2800 kg m<sup>-3</sup> to prepare a quartz concentrate. All samples washed repeatedly in deionised water, and then rinsed three times in acetone. Samples were dried in a 50°C oven for 1 hour prior to dispensing, and then dispensed onto 1 cm diameter 0.25mm thick stainless steel discs sprayed with Electrolube silicone grease. 16 discs per sample were dispensed.

Bulk samples taken from the location of all samples, with the exception of SUTL1435 and 1445, were also dried at 50°C.

### **4.2 Measurements**

#### **4.2.1 Dose Rate Measurements**

Dose rate measurements from the dating samples were undertaken by Thick Source Beta Counting (TSBC), and high resolution gamma spectrometry (HRGS) using the 20g and 50 g dried subsamples and bulk samples referred to above.

Beta dose rates were measured using the SURRC TSBC system (Sanderson, 1988). Sample count rates were determined with 10 replicate 1000s counts for each sample, bracketed by background measurements and sensitivity determinations using the SURRC Shap Granite secondary reference material. Dry infinite-matrix dose rates were calculated by scaling the net count rates of samples and reference material to working beta dose rate of the Shap Granite ( $6.25 \pm 0.03$  mGy a<sup>-1</sup>). The estimated errors combine counting statistics, observed variance and the uncertainty on the reference value.

HRGS measurements were performed using two “n” type hyperpure Ge detectors (EG&G Ortec Gamma-X) operated in a low background lead shield with copper liner. With the exception of samples SUTL1435 and 1445, all samples were sealed in 50mm 185g geometry for a minimum of 2-3 weeks prior to measurement to allow radon equilibration. (Samples SUTL1435 and 1445 were sealed in 50g geometry due to a lack of material). Gamma ray spectra were recorded over the 30 keV to 3 MeV range from each sample, interleaved with background measurements and measurements from Shap Granite in the same geometry. Counting times of 85 ks per sample were used. The spectra were analysed to determine count rates from the major line emissions from <sup>40</sup>K (1457 keV), and from selected nuclides in the U decay series

( $^{234}\text{Th}$ ,  $^{226}\text{Ra}$  +  $^{235}\text{U}$ ,  $^{214}\text{Pb}$ ,  $^{214}\text{Bi}$  and  $^{210}\text{Pb}$ ) and the Th decay series ( $^{228}\text{Ac}$ ,  $^{212}\text{Pb}$ ,  $^{208}\text{Tl}$ ) and their statistical counting uncertainties. Net rates and activity concentrations for each of these nuclides were determined relative to Shap Granite by weighted combination of the individual lines for each nuclide. The internal consistency of nuclide specific estimates for U and Th decay series nuclides was assessed relative to measurement precision, and weighted combinations used to estimate mean activity concentrations (in  $\text{Bq kg}^{-1}$ ) and elemental concentrations (% K and ppm U, Th) for the parent activity. These data were used to determine dry infinite matrix dose rates for alpha, beta and gamma radiation. These were used in combination with measured water contents, field gamma dose rates and TSBC results, and with estimated internal alpha activity and modelled cosmic ray dose rates, used to determine the overall effective dose rates for age estimation.

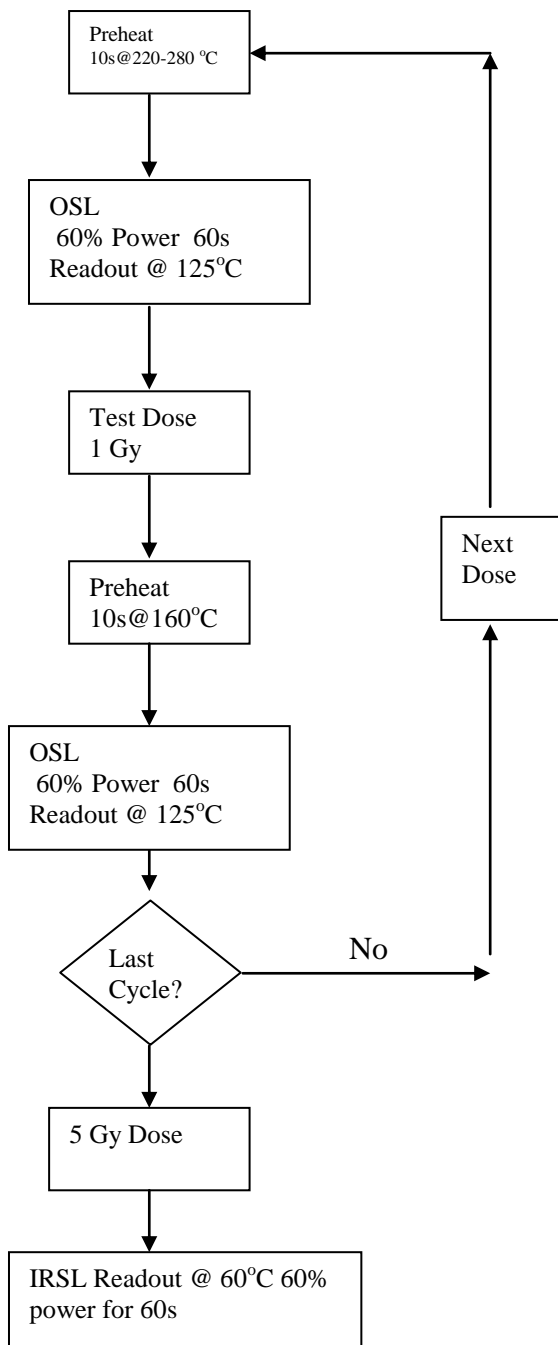
#### 4.2.2 Luminescence measurements

Samples were subjected to a Single Aliquot Regenerative (SAR) procedure following the sequence outlined in figure 4.1. In this procedure measurements of OSL signal levels from individual discs are calibrated to provide stored dose estimates using an interpolated dose-response curve constructed by regenerating OSL signals in the laboratory after each readout cycle. Sensitivity changes which may occur as a result of readout, irradiation and preheating (to remove unstable radiation induced signals) are monitored using a series of small test dose measurements which interleave the sequence of constructing the dose response curve. Stored doses are determined using normalised OSL signals, whereby each measurement is standardised to the test dose response determined immediately after its readout, thus compensating for observed changes in sensitivity during the laboratory measurement cycle. The ability of this procedure to correct for laboratory induced sensitivity changes is assessed using a recycling check whereby a low-dose irradiation near the start of the sequence is compared with a repeat measurement at the end of the sequence.

For OSL dating samples, the natural signal was first read out, followed by a sequence of doses administered to reconstruct the regeneration line. The dose sequence was as follows; 2,4,6,8,10,0,2 Gy. The repeated 2 Gy measurement was used to calculate recycling ratios in order to examine the effectiveness of sensitivity corrections. The zero Gy point at the end was used to monitor whether any residual OSL signals had accumulated over the measurement sequence. In addition, at the end of the run, a 5Gy dose was given, followed by an IRSL readout to check for possible contamination by IR sensitive minerals. 16 discs were dispensed for each sample, with four different preheat temperatures investigated (220, 240, 260 and 280°C), using sets of four discs for each data point. This enabled an assessment to be made of the dependence of equivalent dose ( $D_e$ ) on preheat temperature.

Sample SUTL1439 was later re-run with dose points of 0.1, 0.2, 0.3, 0 and 0.1Gy with a test dose of 0.1Gy when it became apparent that the stored dose of the material was <1 Gy. This repeat measurement improved the overall precision of the sample.

**Fig 4.1: Quartz Single Aliquot Regenerative Sequence**



## 5 Results

### 5.1 Dose Rate Measurements and Calculations

Annual dose rates were estimated from the combination of on-site gamma spectrometry and laboratory measurements by TSBC and HRGS. Whereas field measurements were performed with the moisture content present at time of sampling, all laboratory measurements were conducted on dry samples. Water contents however were measured in the laboratory and used together with water attenuation corrections and microdosimetric grain size attenuation factors to calculate effective dose rates. Whereas the major sources of dose for dating could in principle have been estimated simply on the basis of field gamma spectrometry and TSBC, the addition of HRGS provides opportunities for independent verification of the inferred values, and also to evaluate the composition of the dosimetry in terms of relative contributions from U, Th and K, and sensitivity both to internal and external sources of radiation. The measured values from each technique, and their reconciliation and use to evaluate effective dose rates for 125-250 $\mu$ m quartz are summarised in tabular form below.

Table 5.1 presents HRGS results from each of the eleven dating samples both as activity concentrations ( $\text{Bq kg}^{-1}$ ) and as equivalent concentrations, assuming in the case of the U and Th series full series equilibrium. The data were calibrated with respect to the SURRC secondary Shap Granite sample, and uncertainties have taken account of both analytical errors and the error in the reference values. Mean parent concentrations from all eleven samples were  $0.93 \pm 0.03$  %K,  $0.74 \pm 0.04$  pm U, and  $2.45 \pm 0.05$  ppm Th. These concentrations are lower than for many terrestrial soils, but are not atypical for quartz rich sands, which form the majority of the samples. The mean Th/U concentration ratio of all eleven samples is  $3.31 \pm 0.19$  which is consistent with typical crustal values. The K concentration is slightly higher than typical proportions relative to U and Th, leading to an overall increase in beta dose rate.

Table 5.2 collates dose rates from laboratory and field gamma spectrometry plus thick source beta counting. Whereas the HRGS measurements were conducted with sealed samples which had been stored for radon accumulation, TSBC measurements were conducted in open geometry after drying the sample and would therefore not be expected to retain full equilibrium radon levels. However, the mean ratio of dry infinite-matrix beta dose rates determined by HRGS and TSBC was  $0.97 \pm 0.03$ , indicating little evidence of disequilibrium within these samples.

Table 5.3 presents measured and assumed water content for all samples. It is unlikely that any of the deposits sampled would ever have reached full water content saturation for prolonged periods of time due to the well drained nature of the site. As such, assumed water contents for samples have been estimated to reflect the range of measured actual water contents. Water content corrections have been applied to the average beta dose rate from HRGS and TSBC (Zimmerman, 1971), and to the dry gamma dose rates determined by HRGS. Effective beta dose rates combine water content corrections with grain size attenuation corrections giving results which are broadly similar from sample to sample, with a mean value of  $0.84 \pm 0.03$  mGya<sup>-1</sup>.

**Table 5.1 Activity and Equivalent concentrations of K, U and Th for samples SUTL1435-1445 as determined by HRGS**

Sample (SUTL)	Activity Concentrations /Bqkg <sup>-1</sup>			Equivalent Concentrations <sup>1,2</sup>		
	K	U	Th	K (%)	U (ppm)	Th (ppm)
1435	239±38	4.96±3.47	8.80±2.11	0.77±0.12	0.40±0.28	2.17±0.52
1436	280±6	10.70±0.20	10.30±0.2	0.90±0.02	0.87±0.02	2.54±0.05
1437	266±6	10.25±0.20	9.97±0.12	0.86±0.02	0.83±0.01	2.46±0.03
1438	260±22	8.39±1.07	9.98±0.84	0.84±0.07	0.68±0.09	2.46±0.21
1439	280±6	10.57±0.20	10.14±0.13	0.90±0.02	0.86±0.02	2.50±0.03
1440	348±23	8.18±1.07	10.04±0.84	1.13±0.07	0.66±0.09	2.47±0.21
1441	312±6	10.30±0.20	10.40±0.13	1.01±0.02	0.83±0.02	2.56±0.03
1442	307±23	9.91±1.09	11.41±0.84	0.99±0.07	0.80±0.09	2.81±0.21
1443	324±6	10.08±0.19	10.24±0.13	1.05±0.02	0.82±0.02	2.52±0.03
1444	280±6	7.73±0.17	8.93±0.13	0.91±0.02	0.63±0.01	2.20±0.03
1445	263±38	8.14±3.34	9.24±2.22	0.85±0.12	0.66±0.27	2.27±0.55

1. Conversion factors (based on OECD,1994) : <sup>40</sup>K : 309.26 Bq kg<sup>-1</sup> %K<sup>-1</sup> ; <sup>238</sup>U : 12.34787 Bq kg<sup>-1</sup> ppmU<sup>-1</sup> ; <sup>232</sup>Th : 4.057174 Bq kg<sup>-1</sup> %<sup>-1</sup>.

2. Working values for Shap Granite :4.43+-0.03%K, 12.00+-0.06 ppm U, 28.5+-0.26 ppm Th. In Bq kg<sup>-1</sup>: K- 1370+-10 Bq kg<sup>-1</sup>, U-238 148.17+-7.4 Bq kg<sup>-1</sup>, <sup>232</sup>Th - 115.6+-1.05 Bq kg<sup>-1</sup>. Based on high resolution gamma spectrometry relative to CANMET and NBL standards by from Sanderson, 1986.

**Table 5.2 Dose Rates Determined by HRGS, TSBC and field gamma measurements**

Sample (SUTL)	Dry Infinite Matrix dose rates <sup>1</sup> by HRGS /mGya <sup>-1</sup>			TSBC /mGya <sup>-1</sup> D <sub>β</sub> (dry)	Field γ / mGya <sup>-1</sup> D <sub>γ</sub> (wet)
	D <sub>α</sub> (dry)	D <sub>β</sub> (dry)	D <sub>γ</sub> (dry)		
1435	2.72±0.87	0.76±0.11	0.34±0.05	0.96±0.04	0.32±0.02
1436	4.28±0.06	0.95±0.02	0.45±0.01	0.97±0.07	0.28±0.02
1437	4.12±0.05	0.90±0.02	0.43±0.01	0.89±0.04	0.34±0.02
1438	3.71±0.28	0.87±0.06	0.41±0.02	0.94±0.04	0.28±0.02
1439 <sup>3</sup>	4.23±0.05	0.95±0.02	0.44±0.01	0.88±0.05	0.29±0.02
1440	3.67±0.28	1.10±0.06	0.47±0.02	1.19±0.05	0.31±0.02
1441	4.21±0.05	1.03±0.02	0.47±0.01	1.01±0.04	0.28±0.02
1442	4.31±0.29	1.02±0.06	0.48±0.02	0.95±0.04	0.28±0.02
1443	4.13±0.05	1.06±0.02	0.48±0.01	1.02±0.04	0.27±0.02
1444	3.36±0.04	0.91±0.02	0.40±0.01	0.86±0.06	0.26±0.02
1445	3.51±0.85	0.87±0.11	0.40±0.05	0.87±0.05	0.33±0.02

1. Based on Dose Rate conversion factors from Aitken, 1983.

**Table 5.3 Annual Dose Rates for samples SUTL1435-1445**

Sample SUTL	Water Content			Effective $\beta$ dose rate <sup>1</sup> /mGya <sup>-1</sup>	$D_\gamma$ (wet) by HRGS /mGya <sup>-1</sup>	Effective $\gamma$ dose rate /mGya <sup>-1</sup>	Total dose rate <sup>2</sup> /mGya <sup>-1</sup>
	FW /%	SW /%	Assumed /%				
1435	7.1	39.4	5±5	0.86±0.06	0.33±0.05	0.32±0.03	1.26±0.08
1436	10.9	33.1	5±5	0.83±0.06	0.42±0.02	0.35±0.01	1.37±0.06
1437	3.5	27.9	5±5	0.77±0.05	0.41±0.02	0.37±0.01	1.33±0.05
1438	0.3	21.6	5±5	0.78±0.06	0.39±0.03	0.33±0.02	1.30±0.06
1439	0.1	18.0	5±5	0.78±0.05	0.42±0.02	0.36±0.01	1.32±0.06
1440	6.5	27.9	5±5	1.00±0.07	0.45±0.03	0.38±0.02	1.56±0.07
1441	1.9	21.0	5±5	0.88±0.05	0.45±0.02	0.37±0.01	1.43±0.06
1442	0.1	19.0	5±5	0.86±0.06	0.45±0.03	0.37±0.02	1.41±0.07
1443	0.1	27.2	5±5	0.89±0.06	0.45±0.02	0.36±0.01	1.44±0.06
1444	0.1	23.1	5±5	0.76±0.05	0.38±0.02	0.32±0.01	1.26±0.06
1445	3.0	30.1	5±5	0.75±0.07	0.38±0.05	0.35±0.03	1.29±0.08

1. Effective beta dose rates combine water content corrections with inverse grain size attenuation factors obtained by weighting the 200 micron mean grain size attenuation factors of Mejdahl (1979) for K, U and Th sources by the relative contributions to beta dose rate from each source determined by HRGS.

2. Obtained from the combination of effective beta and gamma dose rates and an additional 0.185 mGya<sup>-1</sup> allowance for the dose rate due to cosmic radiation (Prescott and Hutton, 1994).

Calculated wet gamma dose rate values determined by HRGS are also tabulated. Comparison of these values with on-site gamma measurements show on average HRGS values to be in the region of 40% higher than on-site measurements. This may be due to the influence of lower dose rate material around the sediments sampled, or reflect slight differences in water content during field measurements.

Calculated total effective dose rates vary from 1.26-1.56 mGya<sup>-1</sup>. The overall uncertainties in dose rate combining all data sets and corrections are in the region of 4-6% for all samples. The precision is in part a reflection of the better counting statistics achieved through measurement of large 185g HRGS samples, combined with long counting times for TSBC measurements. The dosimetry of these samples is dominated by beta and gamma contributions from K, with external gamma radiation representing only 20% of the total annual dose rate.

## 5.2 Single Aliquot OSL Results

Data from the single aliquot regenerative dose determinations were analysed both using the Risoe “Analyst” programme, which constructed individual dose response curves and estimated doses for each disc, and using Excel spreadsheets and Jandel Sigmaplot software to examine composite data sets. Each individual measurement was scrutinised for OSL decay shape and signal consistency relative to the other measurements in the sets of upto 16 discs per sample originally examined. Checks for zero level were satisfactory in all cases (representing less than 1% of the test dose response). Checks for IR contamination showed a small number of discs with large IR signal. These were excluded from further analysis. For the majority of samples there was clear evidence that the measured variance of regenerated dose response points (typically reproduced with  $\pm 4-5\%$  or better within groups of discs from the sample sample) was significantly smaller than the distribution of normalised natural OSL signals (which varied from  $\pm 8-12\%$  depending on the sample). This was taken as an indication that the dose response curves from individual discs in each could be treated as random samples from the same underlying form. Moreover there was no evidence of significant differences in normalised OSL ratios (both in natural and regenerated dose points) between the subsets of discs pre-heated at temperatures from  $220^{\circ}\text{C}$  to  $280^{\circ}\text{C}$ . Accordingly composite dose response curves from all discs for each sample were constructed and used to estimate equivalent dose values for each of the individual discs, and their combined sets. Linear fitting was used in determining parameters for the dose response curves, and it was also noted that the coefficients determined from each sample were within statistical limits of each other.

Table 5.4 summarises the SAR characteristics and unweighted results. Clearly the choice of pre-heating temperature does not have a systematic effect on estimated dose.

Table 5.5 summarises age determinations based both on unweighted and weighted combination of data from the individual discs. Error estimates are typically 8-14% for unweighted results. The use of weighted combinations can be seen to significantly reduce the uncertainty on the error measurement with values typically in the region of 2-8%. However, the use of weighted analysis in these samples can be seen to effect the overall ED obtained, with weighted values typically 20% lower than unweighted.

**Table 5.4 Summary of SAR results from 16 disc runs**

Sample /SUTL	Mean Sensitivity /Counts Gy <sup>-1</sup>	Sensitivity change /% per cycle	Recycling ratio	D <sub>e</sub> at 220°C / Gy	D <sub>e</sub> at 240°C / Gy	D <sub>e</sub> at 260°C / Gy	D <sub>e</sub> at 280°C / Gy	Combined D <sub>e</sub> /Gy	D <sub>e</sub> Precision / %
1435	1000	1.6	1.03±0.08	5.98±0.68	6.69±1.03	3.19±0.60	5.63±0.68	5.52±0.47	8.58
1436	1200	0.8	1.03±0.05	6.79±1.25	5.90±1.00	3.09±0.60	3.71±0.64	4.87±0.61	12.42
1437	350	2.6	1.07±0.08	5.54±0.99	5.37±0.87	6.05±0.71	4.99±0.90	5.49±0.46	8.50
1438	1300	2.2	1.11±0.07	6.04±1.71	5.59±1.52	5.25±1.62	5.27±1.20	5.34±0.81	14.72
1439	600	2.5	1.06±0.08	0.27±0.05	0.26±0.06	0.27±0.07	0.36±0.04	0.28±0.04	13.36
1440	2150	2.0	0.90±0.04	7.92±0.99	7.69±1.33	9.20±3.18	6.52±1.77	7.64±0.84	10.97
1441	1200	1.7	1.01±0.04	6.37±0.81	5.16±0.55	7.64±0.73	5.65±1.10	6.20±0.48	7.78
1442	1100	2.4	1.00±0.04	7.61±1.17	5.39±0.84	5.76±1.27	5.58±0.81	6.08±0.53	8.77
1443	1200	2.3	1.08±0.08	5.90±0.98	6.43±1.11	9.67±2.02	4.81±1.26	6.70±0.80	11.93
1444	1500	1.8	1.00±0.06	8.82±2.31	5.64±0.58	5.21±0.82	4.56±1.02	6.06±0.76	12.47
1445	2100	2.4	0.99±0.02	6.54±0.31	6.88±0.47	5.62±1.42	4.47±1.16	5.88±0.50	8.46

**Table 5.5 Summary of age estimates**

Sample /SUTL	Effective Dose Rate/ mGya <sup>-1</sup>	Combined De/ Gy	Age /ka	Weighted De /Gy	Age /ka
1435	1.26±0.08	5.52±0.47	4.38±0.47	3.95±0.07	3.13±0.21
1436	1.37±0.06	4.87±0.61	3.57±0.47	3.76±0.22	2.75±0.20
1437	1.33±0.05	5.49±0.46	4.13±0.38	4.54±0.24	3.41±0.21
1438	1.30±0.06	5.54±0.81	4.26±0.35	6.00±0.51	4.62±0.45
1439	1.32±0.06	0.28±0.04	0.215±0.030	0.24±0.03	0.178±0.021
1440	1.56±0.07	7.64±0.84	4.90±0.58	4.99±0.30	3.20±0.24
1441	1.43±0.06	6.20±0.48	4.34±0.38	4.73±0.20	3.31±0.20
1442	1.41±0.07	6.08±0.53	4.31±0.43	4.97±0.13	3.52±0.20
1443	1.44±0.06	6.70±0.80	4.65±0.59	6.20±0.19	4.31±0.22
1444	1.26±0.06	6.06±0.76	4.81±0.65	5.69±0.15	4.52±0.25
1445	1.29±0.08	5.88±0.50	4.55±0.47	4.92±0.08	3.81±0.24

## 6. Discussion and Conclusions

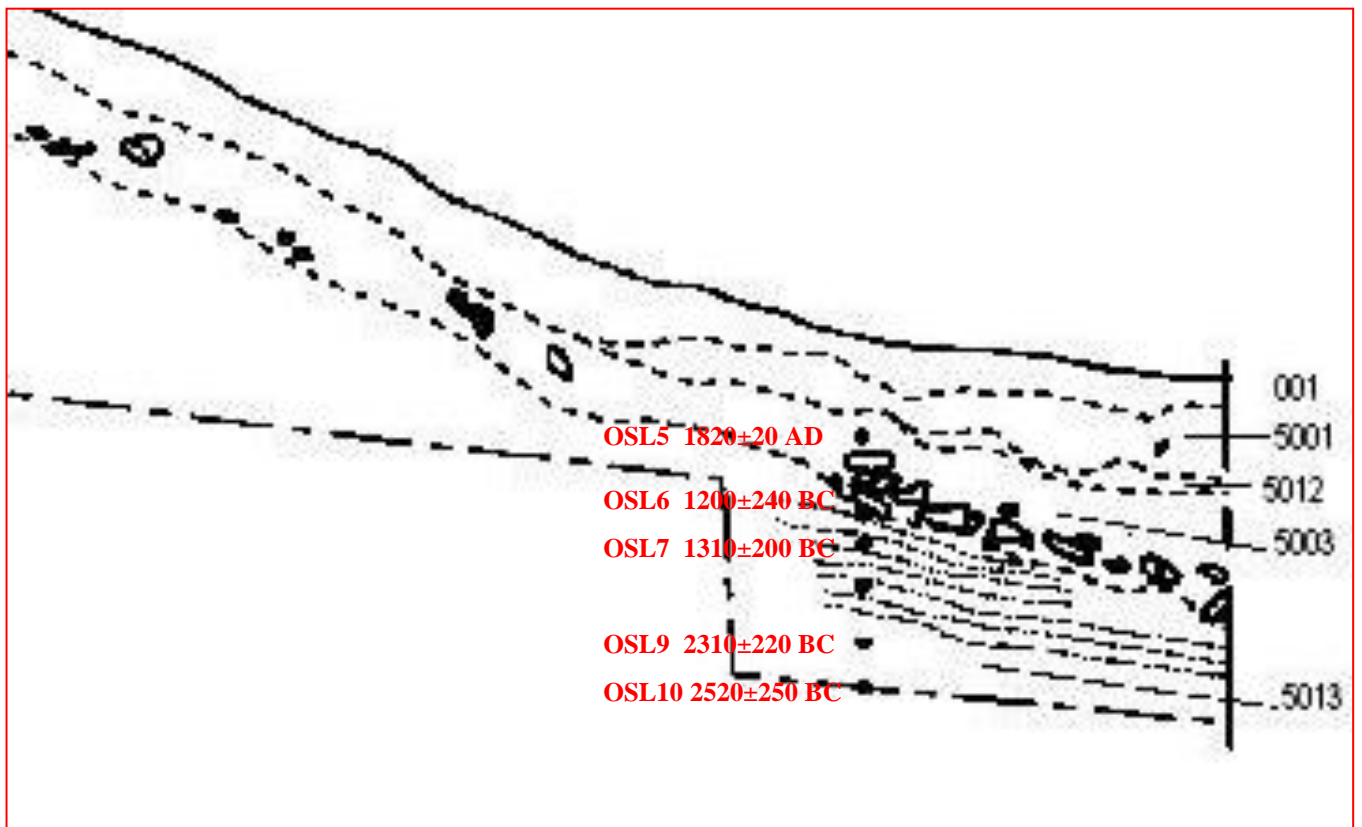
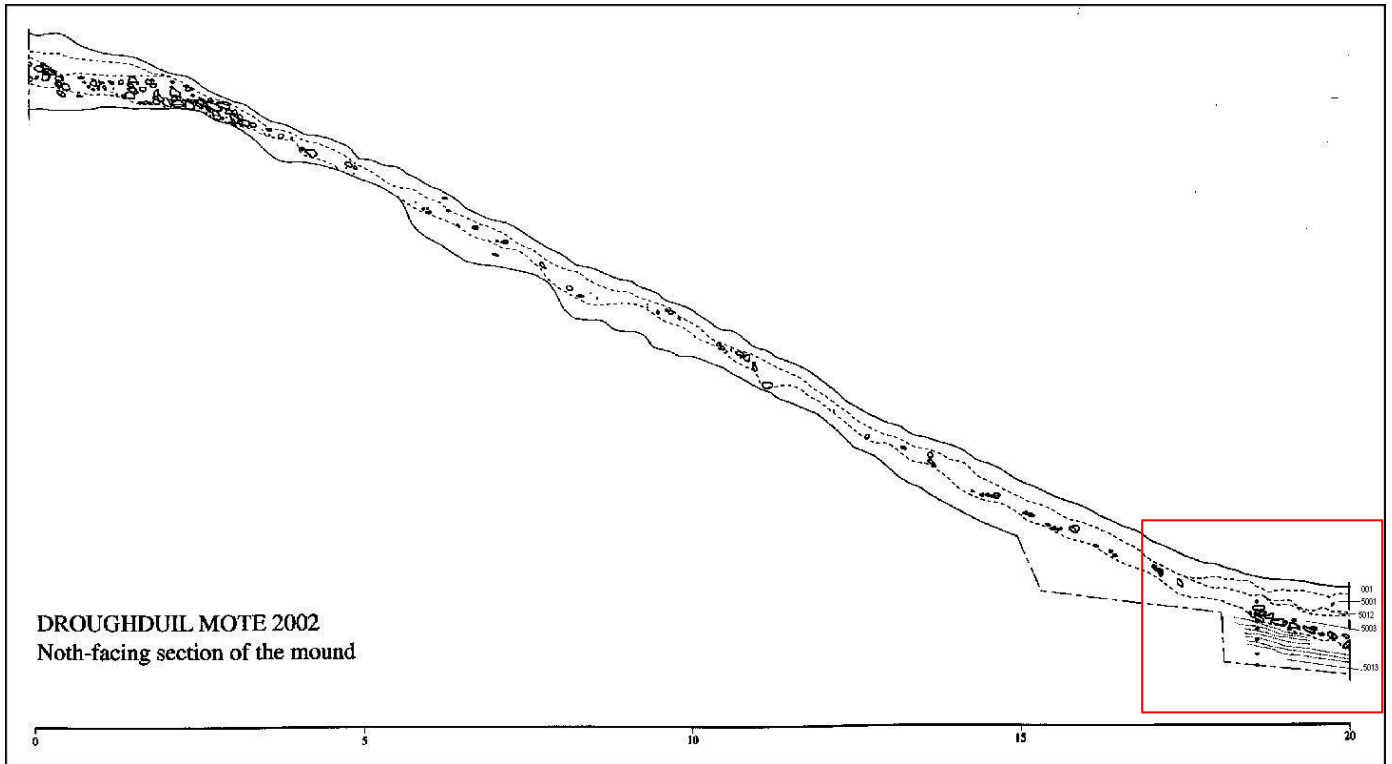
Table 6.1 summarises the final age estimates for samples from Droughduil mound. Samples from the base of the trench which are vertically associated with one another (OSL 5-10/ SUTL 1439-1444) are in stratigraphic order, and suggest the oldest excavated layer associated with the mound to date to the mid 3<sup>rd</sup> millenium BC. Later land surfaces above this layer appear to have formed in the period between 1200-2500 BC before a hiatus in deposition. The next major deposit / landsurface is relatively modern in age, dating to the beginning of the 19<sup>th</sup> Century AD. It is possible that this depositional sequence is therefore related to activity on the site around the time that the observational hut was in use.

Deposits which were thought to predate the cairn construction, indicate a terminus post quem for the cairn construction of around 1800 BC. Dates associated with the majority of deposits from after the cairn collapse suggest that the cairn had gone out of use by 1400BC, though it should be noted that sample OSL4 / SUTL 1438 contradicts this evidence. Indeed the age of OSL 4, 2620±450 BC is the oldest date obtained for the site. Given the sampling position, below rubble and stone, it is possible that this material represents poorly zeroed sediment from an earlier landsurface.

**Table 6.1 Final Age Estimates**

OSL No	Sample /SUTL	Age /ka	Date	Co-ord		Description of Context	Significance
1	1435	3.13±0.21	1130±210 BC	E N	528.328 468.327	10cm beneath cairn	Tpq for cairn
2	1436	2.75±0.20	750±200 BC	E N	528.318 468.340	28cm below cairn	Predates OSL 1
3	1437	3.41±0.21	1410±210 BC	E N	528.250 468.170	Base of cairn in sand/cobbles	Tpq for end of cairn
4	1438	4.62±0.45	2620±450 BC	E N	523.488 466.104	Beneath stones, mound side	Tpq for collapse
5	1439	0.178±0.021	1820±20 AD	E N	511.570 466.077	Bottom profile, above stone layer	Tpq for cairn collapse
6	1440	3.20±0.24	1200±240 BC	E N	511.587 466.074	Below stone layer	Tpq for cairn collapse
7	1441	3.31±0.20	1310±200 BC	E N	511.599 466.090	Below first 'turf' feature – Earlier land surface	Earlier land surface
8	1442	3.52±0.20	1520±200 BC	E N	511.617 466.123	Below 2 <sup>nd</sup> 'turf' feature – Earlier land surface	Earlier land surface
9	1443	4.31±0.22	2310±220 BC	E N	511.642 466.071	Below weathered surface features – Earlier land surface	Earlier land surface
10	1444	4.52±0.25	2520±250 BC	E N	511.632 466.128	Base of Trench- oldest excavated layer	Oldest excavated layer
11	1445	3.81±0.24	1810±240 BC	E N	529.810 467.722	Beneath cairn after quarter sectioning	Beneath cairn after quarter sectioning

**Fig 6.1 North Facing Section of Droughduil mound, indicating position of samples SUTL 1439-1444 and dating results**



## 7. References

- Aitken M.J., 1998. An introduction to optical dating, Oxford Science Publications.
- Aitken M.J., 1983, Dose Rate Data in SI Units, PACT 9, 69-76
- Bell W.T., 1976, Attenuation factors for the absorbed radiation dose in quartz grains for thermoluminescence dating, Ancient TL 8, 2-13
- Bøtter-Jensen, L., Bulur, E., Duller, G.A.T., Murray, A.S., 2000. Advances in luminescence instrument systems. Radiation Measurements 32, 523-528.
- Duller, G.A.T., Bøtter-Jensen, L., Murray, A.S., 2000. Optical dating of single sand-sized grains of quartz: sources of variability. Radiation Measurements 32, 453-457.
- Duncan J, 2003, GUARD 1078 Hilton of Cadboll, Post excavation Phase: Soils Draft Report 13/6/03, University of Glasgow
- James H., 2002, Investigation of the setting and context of the Hilton of Cadboll Cross-slab, Recovery of the stump, and fragment of sculpture, GUARD project 1078, Data Structure report, University of Glasgow.
- Lepper, K., Agersnap Larsen, N., McKeever, S.W.S, 2000. Equivalent dose distribution analysis of Holocene eolian and fluvial quartz sands from Central Oklahoma. Radiation Measurements 32, 603-608.
- Mejdahl, V., 1979, Thermoluminescence dating : beta dose attenuation in quartz grains, Archaeometry, 21(1), 61-72
- Murray, A.S., Wintle, A.G., 2000. Luminescence dating of quartz using an improved single-aliquot regenerative-dose protocol. Radiation Measurements 32, 57-73.
- OECD, 1994, JEF-PC – A personal computer programme for Displaying Nuclear Data from the Joint Evaluated File Library, OECD, Nuclear Energy Agency, Paris.
- Olley, J., Caitcheon, G., Murray, A.S., 1998. The distribution of apparent dose as determined by optically stimulated luminescence in small aliquots of fluvial quartz: implications for dating young sediments. Quaternary Science Reviews (Quaternary Geochronology) 17, 1033-1040.
- Olley, J.M., Caitcheon, G.G., Roberts, R.G., 1999. The origin of dose distributions in fluvial sediments, and the prospect of dating single grains from fluvial sediments using optically stimulated luminescence. Radiation Measurements 30, 207-217.
- Prescott, J.R. and Hutton, J.T., (1994) Cosmic ray contributions to dose rates for luminescence and ESR dating: large depths and long-term time variations. *Radiation Measurements*, **23**, 497-500.

Sanderson, D.C.W., Bishop, P., Houston, I., Boonsener, M., 2001. Luminescence characterisation of quartz-rich cover sands from NE Thailand. *Quaternary Science Reviews* 20, 893-900.

Sanderson D.C.W., 1986, Working values of activity concentrations and absolute concentrations from Shap Granite, Internal results, Luminescence laboratory SURRC.

Sanderson, D.C.W., 1988. Thick Source Beta Counting : a rapid method for measuring beta dose rates, *Nuclear Tracks*, 14, 203-207.

Sanderson, D.C.W., 2001. Luminescence Dating of Anthropogenically reset sediments from archaeological sites, Archsci 2001 Conference Newcastle, Luminescence & ESR Dating Meeting Glasgow, September 2001.

Sanderson, D.C.W., Bishop, P., Stark, M., Spencer, J.Q., 2002. Luminescence dating of anthropogenically reset canal sediments from Angkor Borei, Cambodia. *Quaternary Science Reviews*, 22, 1111-1121

Sommerville, A.A., Sanderson, D.C.W., Hansom, J.D., Housley, R.A., 2001. Luminescence dating of aeolian sands from archaeological sites in Northern Britain: a preliminary study. *Quaternary Science Reviews (Quaternary Geochronology)* 20, 913-919.

Sommerville, A.A., Hansom, J.D., Sanderson, D.C.W., Housley, R.A., 2003 Optically Stimulated Luminescence Dating of Large Storm Events in Northern Scotland, *Quaternary Science Reviews*, 22, 1085-1092.

Spencer, J.Q., Sanderson, D.C.W., Deckers, K., Sommerville, A.A. Assessing mixed dose distributions in young sediments identified using small aliquots and a simple two-step SAR procedure: the *F*-statistic as a diagnostic tool. *Radiation Measurements* 37, 425-431

Zimmermann, D.W., 1971, Thermoluminescent dating using fine grains from pottery, *Archaeometry* 13, 29-52